



Tree Physiology 00, 1–16
doi:10.1093/treephys/tpaa153



Research paper

Eastern US deciduous tree species respond dissimilarly to declining soil moisture but similarly to rising evaporative demand

Sander O. Denham^{1,2,5}, A. Christopher Oishi², Chelcy F. Miniati², Jeffrey D. Wood³, Koong Yi^{1,4}, Michael C. Benson¹ and Kimberly A. Novick¹

¹O'Neill School of Public and Environmental Affairs, Indiana University—Bloomington, 702 N. Walnut Grove Ave, Bloomington, IN 47405, USA; ²USDA Forest Service, Southern Research Station, Coweeta Hydrologic Laboratory, 3160 Coweeta Lab Rd, Otto, NC 28763, USA; ³School of Natural Resources, University of Missouri, 1111 Rollins St., Columbia, MO 65211, USA; ⁴Department of Environmental Sciences, University of Virginia, 291 McCormick Rd, Charlottesville, VA 29904, USA; ⁵Corresponding author (sodenham@indiana.edu)

Received February 23, 2020; accepted November 5, 2020; handling Editor David Whitehead

Hydraulic stress in plants occurs under conditions of low water availability (soil moisture; θ) and/or high atmospheric demand for water (vapor pressure deficit; D). Different species are adapted to respond to hydraulic stress by functioning along a continuum where, on one hand, they close stomata to maintain a constant leaf water potential (Ψ_L) (isohydric species), and on the other hand, they allow Ψ_L to decline (anisohydric species). Differences in water-use along this continuum are most notable during hydrologic stress, often characterized by low θ and high D ; however, θ and D are often, but not necessarily, coupled at time scales of weeks or longer, and uncertainty remains about the sensitivity of different water-use strategies to these variables. We quantified the effects of both θ and D on canopy conductance (G_c) among widely distributed canopy-dominant species along the isohydric–anisohydric spectrum growing along a hydroclimatological gradient. Tree-level G_c was estimated using hourly sap flow observations from three sites in the eastern United States: a mesic forest in western North Carolina and two xeric forests in southern Indiana and Missouri. Each site experienced at least 1 year of substantial drought conditions. Our results suggest that sensitivity of G_c to θ varies across sites and species, with G_c sensitivity being greater in dry than in wet sites, and greater for isohydric compared with anisohydric species. However, once θ limitations are accounted for, sensitivity of G_c to D remains relatively constant across sites and species. While D limitations to G_c were similar across sites and species, ranging from 16 to 34% reductions, θ limitations to G_c ranged from 0 to 40%. The similarity in species sensitivity to D is encouraging from a modeling perspective, though it implies that substantial reduction to G_c will be experienced by all species in a future characterized by higher D .

Keywords: conductance, drought, sap flux, vapor pressure deficit.

Introduction

The ability of plants to survive and function during periods of hydrologic stress is largely governed by stomatal response to declining soil water supply and increasing atmospheric aridity. Declining soil moisture content (θ) reduces the supply of water to the leaves, limiting stomatal function and increasing tensions in the xylem throughout the plant, which if severe enough may trigger embolism (Tyree and Sperry 1989, McDowell et al.

2008). Independently, atmospheric drought, characterized by elevated vapor pressure deficit (D), can also reduce carbon uptake and increase the risk of xylem embolism even when the soil is relatively wet (Oren et al. 1999, McDowell et al. 2008, Grossiord et al. 2020). Stomatal conductance depends on both guard cell and epidermal turgor (Comstock and Mencuccini 1998, Franks et al. 2001), and leaf turgor depends on the balance between loss of water via transpiration and supply

of water to the leaf from the soil (Mott and Parkhurst 1991, Maier-Maercker 1999, Mott and Franks 2001). While D and θ tend to be correlated at weekly and monthly time scales, over shorter time scales (hourly to daily), D can be quite variable due to synoptic-scale fronts and other phenomenon affecting temperature, whereas θ may not change appreciably. In geographic regions where soil water is not usually limited, it is still possible for D to become limiting during periods of high temperature due to high sensitivity of D to air temperature.

A common approach used to characterize species-specific water-use strategies is to classify them on a spectrum of stomatal response to declining soil water potential (Hochberg et al. 2018). Trees that tightly regulate stomatal conductance to maintain leaf water potential (Ψ_L) such that water loss is minimized and carbon uptake is severely reduced are considered more isohydric (i.e., greater stomatal sensitivity to changing environmental condition). Meanwhile, more anisohydric trees allow Ψ_L to drop throughout a period of hydrologic stress, thus maintaining canopy conductance (G_c) and carbon uptake, but with the risk of increased water loss and xylem failure (Roman et al. 2015). Because most plant species exhibit stomatal behavior that falls somewhere between the two ends of the spectrum (Klein 2014, Martinez-Vilalta et al. 2014), the slope (σ) of the relationship over time between mid-day and pre-dawn Ψ_L (a proxy for soil water availability) can be used as a continuous variable to place species along this spectrum (Martinez-Vilalta et al. 2014).

This approach using σ has been widely used (Hochberg et al. 2018, Novick et al. 2019), due in part to its relative simplicity, as well as promising new approaches for classifying isohydry from remote sensing data (Konings and Gentine 2017). However, the framework is challenged by the fact that σ , interpreted as $\partial\Psi_L/\partial\Psi_S$, does not consider the fact that stomata, and by extension Ψ_L , are also sensitive to D (Tardieu and Simonneau 1998). This is problematic because we know that D is an important independent driver of stomatal closure (Osonubi and Davies 1980, Oren et al. 1999, Grossiord et al. 2020), and neglecting to account for D effects on stomatal conductance and Ψ_L limits the usefulness of the isohydric framework across broad eco-climatic gradients (Novick et al. 2019). The influence of D may also explain why σ has been observed to change as soils dry, leading to apparent shifts in isohydry (Hochberg et al. 2018). Moreover, in some sites where soil water is rarely limiting (but D may still vary substantially), quantifying σ is difficult because the range of soil water is too narrow to elicit a response. These challenges are relevant for eastern US deciduous forests, which are expected to experience warming-induced increases in D across the region (Ficklin and Novick 2017) and small, geographically variable increases in θ (Berg et al. 2017) following precipitation patterns.

Ultimately, understanding the independent stomatal responses to θ and D is important for resolving conceptual challenges

to the isohydric framework, which is otherwise quite popular and embedded in new plant hydraulics modeling schemes that are rapidly being proliferated into land-surface models (Kennedy et al. 2019, Mirfenderesgi et al. 2019). Moreover, understanding the extent to which θ and D sensitivities are coordinated across species and sites is important for understanding future plant drought responses, as these two types of hydrologic stress are expected to become more decoupled in the future. Large and relatively homogeneous increases in D are expected everywhere (Ficklin and Novick 2017), whereas changes in θ will be more variable across the landscape, increasing in some areas and decreasing in others (Berg et al. 2017). Understanding how different, co-occurring tree species respond to soil water deficit versus atmospheric drought is thus fundamental for understanding ecosystem responses to changing climate conditions.

Our first objective is to determine whether species-specific stomatal sensitivities to D vary with θ conditions and whether the species-level coordination of D and θ sensitivities is generalizable across a climate gradient. We will quantify reductions in G_c attributed to D of different tree species under various θ conditions and answer the questions: how does stomatal sensitivity to D vary with θ within and across sites, and what proportion of stomatal limitation is attributed to D and to θ for key tree species growing in different moisture conditions? A substantial body of research performed in well-watered conditions demonstrates that stomatal sensitivities to D are similar across species when θ is non-limiting (Oren et al. 1999). Our study will be focused on understanding if this coordination persists during periods of hydrologic stress (Meinzer et al. 2013). Isohydric behavior is generally understood to function, at least in part, to prevent the occurrence of dangerously low leaf water potentials that could drive xylem failure (Tyree and Sperry 1989, Choat et al. 2012). Because both declining soil moisture and rising D will depress leaf water potential, we hypothesize that plants whose stomata are more sensitive to θ are also particularly sensitive to D because these plants close stomata to maintain a more constant Ψ_L under hydrologic stress. This prediction is also consistent with some of the earlier interpretations of the isohydric concept, which considered the dual role of changing soil moisture and D on leaf water potential dynamics (Tardieu and Simonneau 1998).

Our second objective is to determine if the sensitivity of G_c to D varies in a predictable way across species. We will focus our attention on understanding if the sensitivity of G_c to D depends on θ content. We will quantify how much of the overall limitation to G_c during the growing season is driven by D or by θ dynamics for key eastern US tree species and, moreover, investigate coordination between the sensitivity of G_c and Ψ_L to these variables. We will address these knowledge gaps across a hydro-climatological gradient from North Carolina to Missouri using sap flux, which is particularly useful for our objective because

Table 1. Site descriptions. MAT, mean annual temperature; MAP, mean annual precipitation.

	CWT	MMS	MOZ
Sample period	2005–06	2011–13	2017–18
MAT (°C)	12.9	11.2	12.1
MAP (mm)	1800	1030	986
Common tree species	<i>Carya</i> spp., <i>Liriodendron tulipifera</i> , <i>Quercus prinus</i> , <i>Quercus rubra</i>	<i>Acer saccharum</i> , <i>Liriodendron tulipifera</i> , <i>Quercus</i> spp.	<i>Acer saccharum</i> , <i>Carya ovata</i> , <i>Juniperus virginiana</i> , <i>Quercus alba</i>
Tree heights	37–40 m	27 m	17–20 m
Stand age	~120 years	~80 years	~80 years
Sensor type	Granier thermal dissipation	Compensation heat pulse	Granier thermal dissipation
No. of samples	2 individuals/species; 2 sensors/tree	2 individuals/species; 2 sensors/tree	4 individuals/species; 2 sensors/tree

it is collected at a temporal frequency (e.g., hourly) at which θ and D dynamics are largely decoupled (Novick et al. 2016).

Materials and methods

Site descriptions

Measurements were made at three sites along a hydroclimatic gradient from North Carolina to Missouri (Table 1). Watershed 18, of the USDA Forest Service Coweeta Hydrologic Laboratory (CWT), located in Macon County, North Carolina, is a low-elevation, mixed hardwood, forested reference watershed that has been unmanaged since being selectively logged in the early 1900s (Swank et al. 1988). We used data presented in Ford et al. (2011) for species including *Liriodendron tulipifera* L. (LITU), *Carya* spp. (CASP), *Quercus montana* L. (QUPR) and *Quercus rubra* L. (QURU).

Morgan Monroe State Forest (MMS, AmeriFlux site code US-MMS), located in Monroe County, Indiana, is a secondary deciduous broadleaf forest with 75% of the basal area comprised *Acer saccharum* Marsh. (ACSA), *L. tulipifera* and *Quercus* spp. (QUSP). Compared with CWT, MMS is somewhat cooler and receives substantially less precipitation.

The Missouri Ozark AmeriFlux Site (MOZ, AmeriFlux site code US-MOZ), is located at the University of Missouri's Bassett Wildlife Research and Education Area, in a ~80-year-old, second-growth, upland oak–hickory forest (Wood et al. 2018). Collectively, *Q. alba* (QUAL), *Carya ovata* (CAOV), *A. saccharum* (ACSA) and *Juniperus virginiana* (JUVI) account for ~62% of the stand basal area. Compared with MMS, MOZ is slightly warmer and somewhat drier. For more detailed climate information for each site, see Table 1.

In order to facilitate our understanding of tree responses to soil moisture and atmospheric condition, datasets used spanned years that included average, wet and drought conditions. MMS experienced an exceptional drought in 2012 during the growing season, when it only received 23 mm of rainfall during June and July, which is less than 10% of the long-term mean rainfall (Yi et al. 2017). MOZ also experienced a substantial drought in

2018 with a mean July θ of 22.1%, close to that of the severe 2012 drought when mean July θ was 21.8%. In CWT, the 2005 growing season precipitation was 46% higher than the 67-year average, followed by the 2006 growing season precipitation that was 33% lower than the 67-year average, resulting in low soil moisture. While lower plots maintained mean growing season θ of $\geq 24\%$, upper plots had mean θ of 21 and 12% respectively (Ford et al. 2011).

Theoretical considerations

Understanding the coordination between stomatal sensitivity to soil moisture and D In general, G_c decreases non-linearly with increasing D (Massman and Kaufmann 1991, Monteith 1995), which can be described using a quasi-empirical function (Oren et al. 1999):

$$G_c = b - m \times \ln(D) \quad (\text{mmol m}^{-2} \text{ s}^{-1}) \quad (1)$$

When using Eq. (1), the b represents the conductance when $D = 1.0$ kPa and has been demonstrated to decline as soil water declines (Novick et al. 2016). The m is the sensitivity of G_c to D (i.e., $dG_c/d\ln(D)$). The absolute magnitude of G_c , as well as the magnitude of m and b , is sensitive to cross-site variation in the well-watered conductance rate driven by species, stand structure and soil properties. Thus, when evaluating the relative limitation of G_c by D versus θ , it is useful to normalize the conductance time series to minimize cross-site variations linked to slowly evolving drivers like canopy and soil structure. In this study, to facilitate comparisons of the G_c sensitivity to θ and D across species and sites, we normalized the G_c time series by the mean G_c that was observed during both well-watered conditions (i.e., θ within 80% of field capacity) and D of 1.0 ± 0.2 kPa. As a result, throughout, G_c is presented as a unitless quantity usually constrained between 0 and 1. In some cases, the species maximum G_c corresponds to the second wettest soil moisture bin, so when the data are normalized (by the max G_c of the wettest soil bin), the normalized values of the second wettest quintile are >1 . However, for consistency, we maintain normalization of G_c using data from

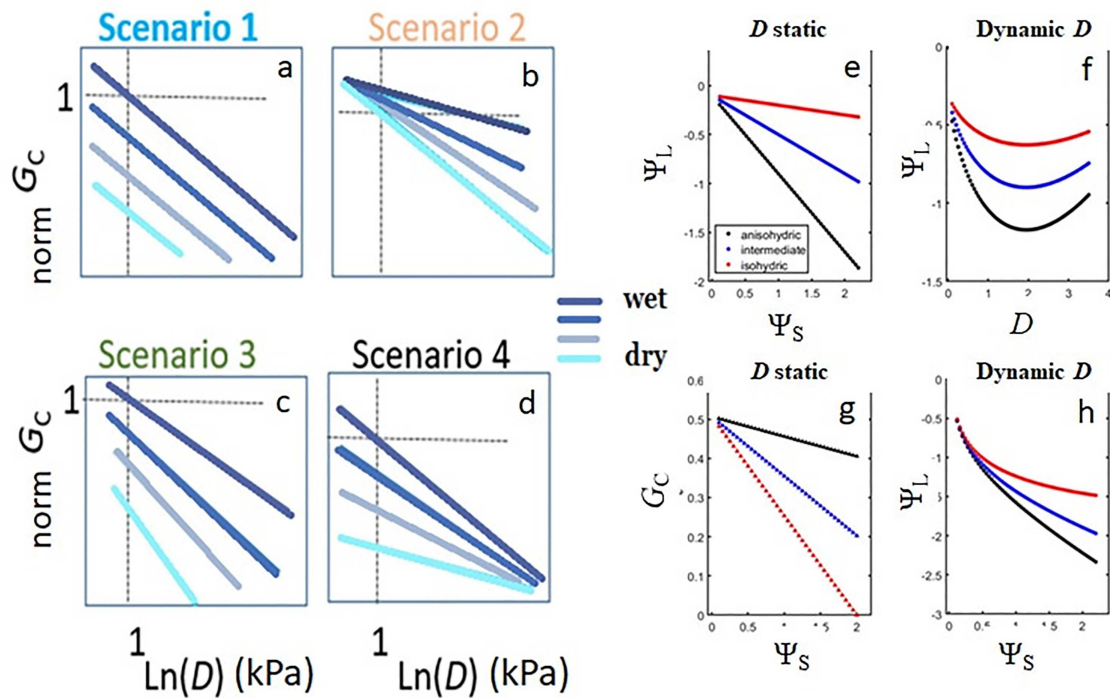


Figure 1. Conceptual illustration of plausible linkages between the stomatal sensitivity to soil moisture and D . Scenarios (panels a–d) are described in the ‘Theoretical considerations’ section. In the typical view of isohydricity, with D assumed to be static, the Ψ_L declines linearly as a function of Ψ_S (e, more anisohydric species have steeper slopes, black line), and G_c is a linear function of Ψ_S (g) with isohydric species (red line) having the steeper slope than anisohydric (black line) species (traditional view). When dynamic D is considered (i.e., via Eq. (4)), stomatal closure under high D causes the relationship of Ψ_L and D to become non-linear at high D (f). Likewise, the relationship between Ψ_L and Ψ_S also becomes non-linear as the soil becomes increasingly dry if D also rises as soils dry (h).

the wettest soil moisture bin rendering a G_c value >1 in some situations.

Oren et al. (1999), and many subsequent studies, have shown that under well-watered conditions, the relationship between m and b across sites and species is well conserved, and linear, with a slope of ~ 0.6 . In other words, during well-watered conditions, $m/b \sim 0.6$ despite variations in growth form or habitat (Domec et al. 2009, Gao et al. 2015, Renninger et al. 2015). Theoretical explanations for this result presume that stomatal regulation keeps Ψ_L near a constant value (consistent with isohydric behavior) but does not specify expected results for species with hydraulic strategies that allow their Ψ_L to decline as soil dries or D increases.

To disentangle D from θ effects, we stratified the normalized G_c time series sets into five quintiles based on θ (Figure 1). For each θ quintile, Eq. (1) was fit to normalized G_c and D observations, yielding in total, five parameter sets for each site species: $b_i = b_1, \dots, b_5$ and $m_i = m_1, \dots, m_5$, where i indexes the quintile (henceforth, bin). These parameters tell us, in a relative sense, how θ and D affect b and m seen in the change in intercept and slope of the $G_c - D$ relationship. Furthermore, understanding how the m parameter changes across the θ bins, and in relation to b , will help us understand how θ and D sensitivities are coordinated.

Our interpretation of variations in m and b is informed by the consideration of four idealized scenarios, illustrated in Figure 1a–d:

Scenario 1: Declining θ reduces b , but G_c sensitivity to D remains unchanged (i.e., m is constant as soils dry, Figure 1a).

Scenario 2: θ does not directly affect stomatal conductance (i.e., constant intercept), but the sensitivity of G_c to D (i.e., m) increases as θ declines (Figure 1b). This scenario may be especially relevant for anisohydric species where G_c is largely unaffected by declining soil water.

Scenario 3: Declining θ reduces b and increases m (Figure 1c).

Scenario 4: Declining θ reduces b but also decreases m (Figure 1d). Only under Scenario 4 is it possible for the ratio $m/b = 0.6$ to be conserved as soils dry.

Determining the extent to which conductance is ultimately limited by soil moisture or D Following the approach from Novick et al. (2016), we estimated the total, growing-season average limitation to G_c attributable to θ and D separately for each species. For every half-hourly data point, the degree of limitation (θ_{lim}) to G_c from θ was calculated as:

$$\theta_{lim} = \frac{(b_{ww} - b_i)}{b_{ww}} \quad (2)$$

where b_i is the intercept for the i_{th} θ bin to which the specific data point belongs, and b_{www} is the intercept for the wettest θ bin (well-watered, bin 5). The relative limitation to G_c from D was then calculated, again for each half-hourly data point, as:

$$D_{lim} = \frac{(b_i - G_c)}{b_{www}} \quad (3)$$

where G_c is the observed normalized G_c for each half hour. When using Eq. (3) to predict G_c (with the bin-specific b_i and m_i), Eq. (3) can then be expressed as:

$$D_{lim} = \frac{(b_i - (b_i - m_i \ln(D)))}{b_{www}} = \frac{m_i \ln(D)}{b_{www}} \quad (4)$$

Extending the analysis to the dynamics of leaf water potential We characterized the degree of isohydricity, following [Martinez-Vilalta et al. \(2014\)](#), using the slope of the relationship between mid-day Ψ_L to Ψ_S (σ_S):

$$\sigma_S = \frac{\partial \Psi_L}{\partial \Psi_S} \quad (5)$$

where the pre-dawn Ψ_L was used as a proxy for plant available Ψ_S ([Améglio et al. 1999](#)).

We also considered an expanded perspective on isohydry, following the approach of [Novick et al. \(2019\)](#), that recognizes the potential for independent variation in mid-day Ψ_L linked to stomatal sensitivity to D . Mathematically, this expanded framework is similar to that presented by [Martinez-Vilalta et al. \(2014\)](#), beginning with the equation relating the transpiration flux of water through a plant stem (T) to the product of G_c and VPD, which in turn is directly related to the product of the whole-plant hydraulic conductance (K) and the soil-to-leaf water potential difference via ([Whitehead et al. 1984](#)):

$$T = G_c \bullet VPD = K (\Psi_S - \Psi_L - \rho gh) \quad (6)$$

where ρgh represents gravity induced head losses. Eq. (6) can be rearranged as an expression for Ψ_L :

$$\Psi_L = \Psi_S - \frac{G_c \times VPD}{K} - \rho gh \quad (7)$$

Next, we again rely on the model of [Oren et al. \(1999\)](#), rearranging it slightly:

$$G_c = b \left[1 - \left(\frac{m}{b} \right) \times \ln(D) \right] \quad (8)$$

noting again that under well-watered conditions at least, the m/b is expected to be ~ 0.6 . Following the approach of [Martinez-Vilalta et al. \(2014\)](#), we then allow both the intercept parameter b and the hydraulic conductivity K , to vary as a function of Ψ_S . Specifically, $b = g_{ref} \bullet f_G(\Psi_S)$ and $K = K_{ref} f_K(\Psi_S)$, where g_{ref}

and K_{ref} are well-watered values. Thus, Eq. (7) becomes:

$$\Psi_L = \Psi_S - \frac{g_{ref} \times f_G(\Psi_S) \times \left(1 - \frac{m}{b} \times \ln(D) \right) \times D}{K_{ref} \times f_K(\Psi_S)} - \rho gh \quad (9)$$

Following arguments presented in both [Martinez-Vilalta et al. \(2014\)](#) and [Novick et al. \(2019\)](#), the $f_G(\Psi_S)$ and $f_K(\Psi_S)$ are collapsed into a single soil water potential sensitivity function representing the combined influence of declining soil water on stomatal function and hydraulic conductivity:

$$\frac{f_G(\Psi_S)}{f_K(\Psi_S)} = 1 + c_{gk} \Psi_S \quad (10)$$

Finally, we introduce a constant α representing the ratio of g_{ref} to K_{ref} , which are both assumed to be constant over the time scales over which drought evolves. Likewise, we neglect the ρgh term, which also should be static over weekly to monthly time scales in forested ecosystems. Thus, the model becomes:

$$\Psi_L = \Psi_S - \alpha \times \left(1 - \frac{m}{b} \times \ln(D) \right) \times (1 + c_{gk} \times \Psi_S) \times D \quad (11)$$

To reiterate, the primary difference between our model and the [Martinez-Vilalta et al. \(2014\)](#) model is the fact that we acknowledge explicitly that conductance depends on D . For this reason, when analyzing the empirical results, we also calculate a complementary variable describing the sensitivity of mid-day Ψ_L to D (σ_D), using the relationship between mean daily D (between hours 12:00–15:00 LDT) and mid-day Ψ_L .

$$\sigma_D = \frac{\partial \Psi_L}{\partial D} \quad (12)$$

This model can be used to understand how coordination of stomatal response to soil moisture and D ultimately affects the dynamics of leaf water potential. When variation in an isolated function of D is neglected (as is often the case when characterizing isohydry), the Ψ_L of more anisohydric species decreases linearly as Ψ_S declines while more isohydric species maintain Ψ_L within a narrow range ([Figure 1e](#)). This is because G_c of isohydric species declines linearly as Ψ_S declines while more anisohydric species maintain more stable G_c with decreasing Ψ_S ([Figure 1g](#)). Nevertheless, if we allow D to increase over time, Ψ_L might initially decline linearly, but recover as stomata close at high D ([Figure 1f](#)). Therefore, when D varies in coordination with θ (i.e., increasing D as θ declines), and the stomatal response to D is considered, the relationship between Ψ_L and Ψ_S also becomes non-linear ([Figure 1h](#)). In other words, stomatal sensitivity to D may explain some of the apparent 'shifts' in σ_S as drought progresses as described in [Hochberg et al. \(2018\)](#).

Sap flux measurements

Compensation heat pulse method—MMS At MMS, sap flux density was measured for three canopy-dominant species—ACSA, LITU and QUSP—from 2011 to 2013, using the compensation heat pulse method (Green et al. 2003). Two trees of similar diameter were measured for each species, and the range of diameters at breast height (DBH) for each species were 41.2–43.8, 62.7–62.8 and 37.5–44.6 cm for ACSA, LITU and QUSP, respectively. Sapwood annuli were determined by visually examining increment cores collected from each tree. The allometric relationships between DBH and sapwood area proposed by Wullschleger et al. (2001) were used when the visual approach was not suitable. Sapwood radii were 10.9–11.5, 10.2 and 2.0–2.1 cm for ACSA, LITU and QUSP, respectively. We grouped the oaks together because previous analyses comparing red and white oaks revealed high similarity among these species in terms of the magnitude of sap flux density and its variation over time (Yi et al. 2017) and the response of g_s to D did not differ significantly among the two species (Roman et al. 2015). The probes and heaters used were manufactured specifically for this experiment (Tranzflo NZ Ltd, Palmerston North, Manawatu-Wanganui, New Zealand). See Yi et al. (2017) for further details. Areas around the probe insertion points were protected with foam blocks wrapped with reflective insulation (Reflectix, Markleville, IN, USA) to shield probes from solar radiation, thermal gradients and rainfall.

Corrected heat pulse velocity (V_C) was converted to J_s according to: $J_s = (0.441 \times F_{\text{wood}} + F_{\text{water}}) V$; where F_{wood} is the volume fraction of wood, F_{water} is the volume fraction of water and V is the raw heat pulse velocity (Dragoni et al. 2009, Yi et al. 2017). G_c was estimated from the measured sap flux using a simplified Penman-Monteith equation: $G_c = \frac{J_s \times \rho_w \times \gamma \times \lambda}{\rho_a \times C_p \times D}$, where J_s is sap flux ($\text{m}^3 \text{m}^{-2} \text{s}^{-1}$), ρ_w is density of liquid water (1000 kg m^{-3}), γ is psychrometric constant (kPa K^{-1}), λ is latent heat of vaporization (J kg^{-1}), ρ_a is density of dry air (kg m^{-3}), C_p is specific heat capacity ($1006 \text{ J kg}^{-1} \text{K}^{-1}$) and D is the vapor pressure deficit of the atmosphere (kPa).

Thermal dissipation probe method—CWT and MOZ At CWT and MOZ, thermal dissipation probes (Granier 1987) were used to determine sap flux density of the outer 1, 2 or 3 cm of the functional xylem at ~ 1.3 m height. For each monitored tree, a pair of sensors was installed circumferentially at least 90° apart. Areas around the probe insertion points were protected as described above. Sap flux (J_s) was calculated using Granier's empirical equation (1987): $J_s = 119 \times 10^{-6} \left(\frac{\Delta T_M - \Delta T}{\Delta T} \right)^{1.231}$, where ΔT_M is the maximum and ΔT is the measured temperature difference between heated and reference probes. Methods are fully described in Ford et al. (2011).

At all sites, areas around the probe insertion points were protected with foam blocks wrapped with reflective insulation

(Reflectix) to shield the probes from solar radiation, thermal gradients and rainfall.

Meteorological data

In CWT, meteorological data were measured in an open-field climate station and from a relative humidity/temperature sensor in the canopy. θ was measured using water content reflectometry probes (CS615 and CS616; Campbell Scientific Inc., Logan, UT, USA) within the top 0–30 cm of soil depth. A soil core was removed from the appropriate depth in soils adjacent and was used to calibrate period output from the sensors to known volumetric water content in the laboratory (Ford et al. 2011). For MMS and MOZ, meteorological data were recorded on the flux tower, including air temperature ($^\circ\text{C}$), atmospheric pressure (P , kPa), relative humidity (RH, %) and photosynthetically active radiation (PAR, W m^{-2}). θ was measured using water content reflectometry probes within the top 0–30 cm of soil (CS615 and CS616; Campbell Scientific Inc.). At MMS, soil moisture at depth (>30 cm) was measured using an EnviroSMART soil water content probe (Sentek Technologies, Stepney, Australia) beginning in April 2006 and was used to derive a weighted Ψ_S down to 50 cm ($\Psi_{S,0-50}$) by scaling the robust shallow measurements by the relative differences observed at deeper depths. This allowed us to characterize the soil water availability across a wider portion of the rooting zone (Roman et al. 2015). D was calculated from the measured RH and temperature. We only used the records measured under conditions of $D \geq 1.0$ kPa because the inferred G_c becomes unreliable when D is very low (Oren et al. 1999).

Leaf water potential (Ψ_L)

We measured Ψ_L using a Scholander-type pressure system (Model 615 PMS pressure chamber, PMS Instrument Company, Albany, OR, USA). At MMS and MOZ, the Ψ_L data were collected contemporaneously with the sap flux data. At CWT, Ψ_L was not measured at the time the sap flux data were installed (2005–2006); instead, Ψ_L was monitored later for the same species growing within 10 km of the site of the original sap flux study. For this reason, we restrict our use of the CWT Ψ_L data to analysis of the sensitivity of Ψ_L to soil moisture and D . We do not explicitly link the CWT Ψ_L data to the CWT sap flux.

While the number and duration of the Ψ_L observations varied from one site to the next, the approach was similar across all three sites. At MMS, one leaf from each tree canopy was covered with aluminum foil for 15 min to allow the Ψ_L to the leaf cells and xylem to equilibrate and prevent biases related to leaf excision (Roman et al. 2015). In general, pre-dawn Ψ_L measurements ($\Psi_{L,PD}$) were collected between 03:00 and 06:00 LDT and were used as a proxy for Ψ_S . Midday Ψ_L measurements ($\Psi_{L,MD}$) were collected between 12:00 and 14:30 LDT. For each sampling week ($n = 64$) during the study, five sunlit leaves (accessed via boom lift) from three individuals of each species

Table 2. Parameter estimates and confidence intervals for $G_c - D$ using the Oren model. Parameters were considered different if confidence intervals did not overlap.

Sites	Species	b	CI (lower, upper)	m	CI (lower, upper)		
CWT	<i>LITU</i>						
	<i>Bin 1</i>	0.89	(0.82, 0.97)	-0.40	(-0.55, -0.25)		
	<i>Bin 2</i>	0.94	(0.82, 1.05)	-0.35	(-0.54, -0.15)		
	<i>Bin 3</i>	0.83	(0.71, 0.94)	-0.22	(-0.40, -0.04)		
	<i>Bin 4</i>	0.92	(0.67, 1.17)	-0.47	(-1.25, 0.30)		
	<i>Bin 5</i>	1	(0.69, 1.31)	-0.73	(-1.50, 0.039)		
	<i>CASP</i>						
	<i>Bin 1</i>	1.04	(0.92, 1.17)	-0.50	(-0.71, -0.29)		
	<i>Bin 2</i>	1.06	(0.93, 1.19)	-0.57	(-0.77, -0.36)		
	<i>Bin 3</i>	1.04	(0.86, 1.22)	-0.51	(-0.80, -0.21)		
	<i>Bin 4</i>	1.28	(1.03, 1.53)	-0.95	(-1.59, -0.31)		
	<i>Bin 5</i>	1	(0.65, 1.34)	-0.56	(-1.33, 0.21)		
	<i>QUPR</i>						
	<i>Bin 1</i>	1.41	(1.28, 1.55)	-0.84	(-1.07, -0.62)		
	<i>Bin 2</i>	1.17	(0.96, 1.39)	-0.65	(-0.99, -0.31)		
	<i>Bin 3</i>	1.28	(1.00, 1.55)	-0.73	(-1.18, -0.27)		
	<i>Bin 4</i>	1.37	(1.16, 1.58)	-0.75	(-1.10, -0.40)		
	<i>Bin 5</i>	1	(0.66, 1.34)	-0.41	(-1.16, 0.34)		
	<i>QURU</i>						
	<i>Bin 1</i>	1.04	(0.93, 1.16)	-0.59	(-0.78, -0.39)		
	<i>Bin 2</i>	1.11	(0.99, 1.23)	-0.68	(-0.87, -0.49)		
	<i>Bin 3</i>	1.20	(1.13, 1.26)	-0.78	(-0.88, -0.67)		
	<i>Bin 4</i>	1.06	(0.96, 1.15)	-0.65	(-0.80, -0.49)		
	<i>Bin 5</i>	1	(0.69, 1.30)	-0.43	(-1.11, 0.25)		
	MMS	<i>LITU</i>					
		<i>Bin 1</i>	0.40	(0.37, 0.43)	-0.25	(-0.28, -0.22)	
		<i>Bin 2</i>	0.74	(0.60, 0.87)	-0.49	(-0.62, -0.35)	
		<i>Bin 3</i>	0.88	(0.79, 0.95)	-0.64	(-0.74, -0.54)	
		<i>Bin 4</i>	0.70	(0.36, 1.04)	-0.36	(-1.15, 0.43)	
		<i>Bin 5</i>	1	(0.45, 1.68)	-0.45	(-1.86, 0.96)	
		<i>ACSA</i>					
		<i>Bin 1</i>	0.54	(0.50, 0.58)	0.31	(-0.35, -0.27)	
		<i>Bin 2</i>	0.62	(0.56, 0.67)	-0.34	(-0.40, -0.29)	
		<i>Bin 3</i>	0.75	(0.71, 0.79)	-0.48	(-0.53, -0.43)	
		<i>Bin 4</i>	0.94	(0.67, 1.17)	-0.46	(-0.85, -0.06)	
		<i>Bin 5</i>	1	(0.58, 1.53)	-0.49	(-1.58, 0.61)	
		<i>QUSP</i>					
		<i>Bin 1</i>	1.04	(0.98, 1.09)	-0.66	(-0.72, -0.59)	
		<i>Bin 2</i>	1.00	(0.91, 1.06)	-0.56	(-0.65, -0.47)	
		<i>Bin 3</i>	1.05	(0.93, 1.16)	-0.67	(-0.81, -0.53)	
		<i>Bin 4</i>	1.05	(0.94, 1.16)	-0.76	(-0.83, -0.59)	
		<i>Bin 5</i>	1	(-0.04, 2.29)	-0.96	(-3.63, 1.72)	
		MOZ	<i>ACSA</i>				
			<i>Bin 1</i>	0.41	(0.38, 0.44)	-0.22	(-0.26, -0.18)
			<i>Bin 2</i>	0.39	(0.34, 0.45)	-0.17	(-0.24, -0.11)
			<i>Bin 3</i>	0.47	(0.41, 0.53)	-0.25	(-0.32, -0.18)
			<i>Bin 4</i>	0.73	(0.48, 0.97)	-0.26	(-1.25, 0.30)
<i>Bin 5</i>	1		(0.80, 1.20)	-0.46	(-0.69, -0.22)		
<i>CAOV</i>							
<i>Bin 1</i>	0.43		(0.41, 0.46)	-0.22	(-0.25, -0.19)		
<i>Bin 2</i>	0.49		(0.47, 0.52)	-0.26	(-0.29, -0.26)		
<i>Bin 3</i>	0.52		(0.47, 0.48)	-0.29	(-0.35, -0.23)		

Continued

Table 2. Continued

Sites	Species	b	CI (lower, upper)	m	CI (lower, upper)
	Bin 4	0.59	(0.45, 0.73)	-0.37	(-0.53, -0.20)
	Bin 5	1	(0.81, 1.18)	-0.65	(-0.87, -0.43)
	JUVI				
	Bin 1	0.59	(0.55, 0.62)	-0.21	(-0.25, -0.17)
	Bin 2	0.69	(0.65, 0.73)	-0.28	(-0.32, -0.23)
	Bin 3	0.75	(0.67, 0.82)	-0.32	(-0.40, -0.25)
	Bin 4	0.95	(0.86, 1.05)	-0.40	(-0.51, -0.28)
	Bin 5	1	(0.91, 1.08)	-0.50	(-0.61, -0.39)
	QUAL				
	Bin 1	0.34	(0.29, 0.38)	-0.08	(-0.14, -0.03)
	Bin 2	0.49	(0.39, 0.60)	-0.23	(-0.36, -0.11)
	Bin 3	0.66	(0.52, 0.80)	-0.33	(-0.49, -0.17)
	Bin 4	1.15	(0.93, 1.38)	-0.85	(-1.14, -0.55)
	Bin 5	1	(0.86, 1.13)	-0.55	(-0.68, -0.41)

were sampled. At MOZ, $\Psi_{L,PD}$ was routinely measured during each growing season at weekly to bi-weekly intervals for multiple species including ACSA, CAO, JUVI and QUAL (Gu et al. 2015). During 2017 and 2018, $\Psi_{L,MD}$ was also measured for five to six sunlit leaves from two to three individuals for each of these species, using a boom lift to access sunlit leaves.

Statistical analysis

We used analysis of variance (ANOVA) to test for differences in the m (slope) and b (intercept) parameters (Eq. (1)), among site and species. A Tukey post hoc test was also used to determine site- and species-level differences in parameters at a 95% family-wise confidence level. The m parameters (slope of fitted lines) were assumed to be statistically no different than the theoretical 0.6 slope if the theoretical line fell within the 95% confidence intervals around mean parameter estimates of fitted line.

Results

G_c sensitivity to θ and D —general patterns and relationship among model parameters

The sensitivity of G_c to θ varied across species ($F_{8,44} = 2.22$, $P < 0.05$) and sites ($F_{2,44} = 21.72$, $P < 0.01$), reflected as changes in the intercept parameter b with increasing dryness (Table 2 and Figure 2). At CWT, declining θ reduced G_c for LITU, but had little or no effect on other species including CASP, QUPR and QURU (Figure 2). At MMS, low θ during the peak of the 2012 drought substantially reduced G_c for LITU (~60%) and ACSA (~50%). In contrast, we observed no θ limitation to G_c of QUSP. However, at the MOZ site, declining θ reduced G_c in QUAL (~27%), ACSA (40%), CAO (40%) and JUVI (20%). Tukey post hoc tests indicate significant differences between CWT and MOZ ($P < 0.01$) but not CWT and MMS ($P = 0.27$) or MMS and MOZ ($P = 0.11$).

Regardless of the effect of θ on G_c , the ratio m/b was relatively well constrained across sites ($F_{2,44} = 0.34$, $P = 0.68$), species ($F_{8,44} = 1.75$, $P = 0.12$) and soil moisture conditions ($F_{4,44} = 1.41$, $P = 0.24$). When the binned G_c data were normalized by the respective intercepts, the G_c sensitivities to D largely converged (Figure 3). Likewise, among sites and species, G_c sensitivity to D (m) increased proportionally to b . With few exceptions, the line $m/b = 0.6$ (henceforth, 0.6 line) fell within the confidence bounds of the relationship of model parameters (Figure 4), and species appeared to follow the trend of Scenario 4 (Figure 1d) demonstrating a simultaneous decrease in b and m with declining θ . In general, the parameters for the oak species (QUPR, QURU, QUSP) were more likely to diverge from the 0.6 line, somewhat consistent with the expectations of Scenario 2 (Figure 1b), maintaining a mostly constant b and decreasing m with declining θ . The 0.6 line was consistently above the ratio of m/b for JUVI at MOZ.

Across species, at least within a site, the coordination between m and b persists (Figure 5), though only in MMS and MOZ did the 0.6 line fall within the confidence bounds of slope of the relationship between these two parameters. Across sites, species level relationships of model parameters generally conformed to ~0.6; however, for oaks, declining θ only decreased b in MOZ; in other sites, declining θ primarily modified the D sensitivity (m).

Partitioning G_c limitations into θ versus D

The results of θ_{lim} (Eq. (2)) and D_{lim} (Eqs (3) and (4)) suggested that relative impact between θ and D on G_c was different, depending on the sites. In CWT, low θ contributed to ~10% reduction in G_c for LITU, but had no effect on CASP, QUPR and QURU (Figure 6a). In CWT, D decreased G_c by 29, 16, 34 and 31% for LITU, CASP, QUPR and QURU, respectively. In MMS, increasing D was almost equally as important in reducing G_c as θ for isohydric LITU and ACSA, while nearly solely driving the

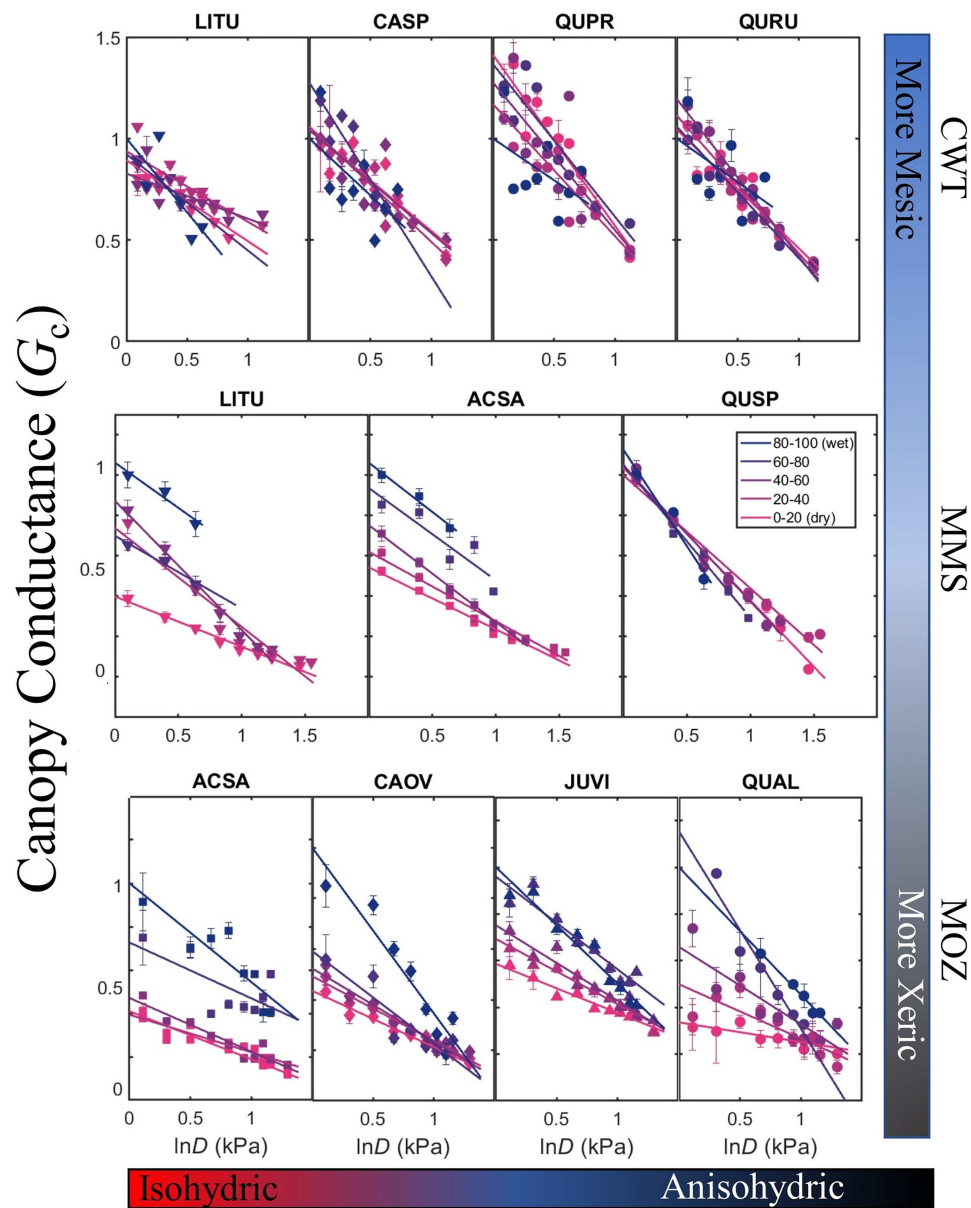


Figure 2. Normalized G_c as a function of the natural log of D binned by θ (%) for each tree species (see text for species codes) at each site. Fitted lines follow the empirical approach of Oren et al. (1999) of each site including CWT (top), MMS (middle) and MOZ (bottom) and showing θ limitations to G_c demonstrated in the variable intercept. Symbol convention is consistent throughout figures: ACSA (square), *Carya* spp. (diamonds), LITU (downward triangle), JUVI (upward triangle) and *Quercus* spp. (circle).

reductions for QUSP. On average, θ limitation resulted in 30, 26 and 5% reductions in G_c for LITU, ACSA and QUSP respectively (Figure 6b), while D explained 20, 20 and 33% reductions in G_c for those same species. Both θ and D were important in reducing G_c for all species in MOZ, with θ explaining 40, 40, 20 and 27% reductions in G_c and D explaining 22, 28, 27 and 34% reductions in G_c for ACSA, CAO, JUVI and QUAL respectively (Figure 7c). We found that θ generally contributed to a larger proportion of the total reduction, moving across the hydroclimatological gradient from more mesic to more xeric, with one important exception being QUSP in MMS.

Coordination of G_c sensitivity to θ and D with isohydricity

Across sites, the ratio m/b did not change, regardless of species Ψ_L sensitivity to Ψ_S (σ_S , $P = 0.36$, Figure 8a) or D (σ_D , $P = 0.57$, Figure 8b). As a result, the species' overall stomatal sensitivity to evaporative demand was predictable from the species' stomatal sensitivity to soil moisture, regardless of the degree of isohydricity. A positive relationship was observed between σ_S and σ_D ($R^2 = 0.77$; $P < 0.002$, Figure 7c). In other words, the Ψ_L of more anisohydric species (e.g., high σ_S) was also generally more sensitive to fluctuations in D (e.g., high σ_D).

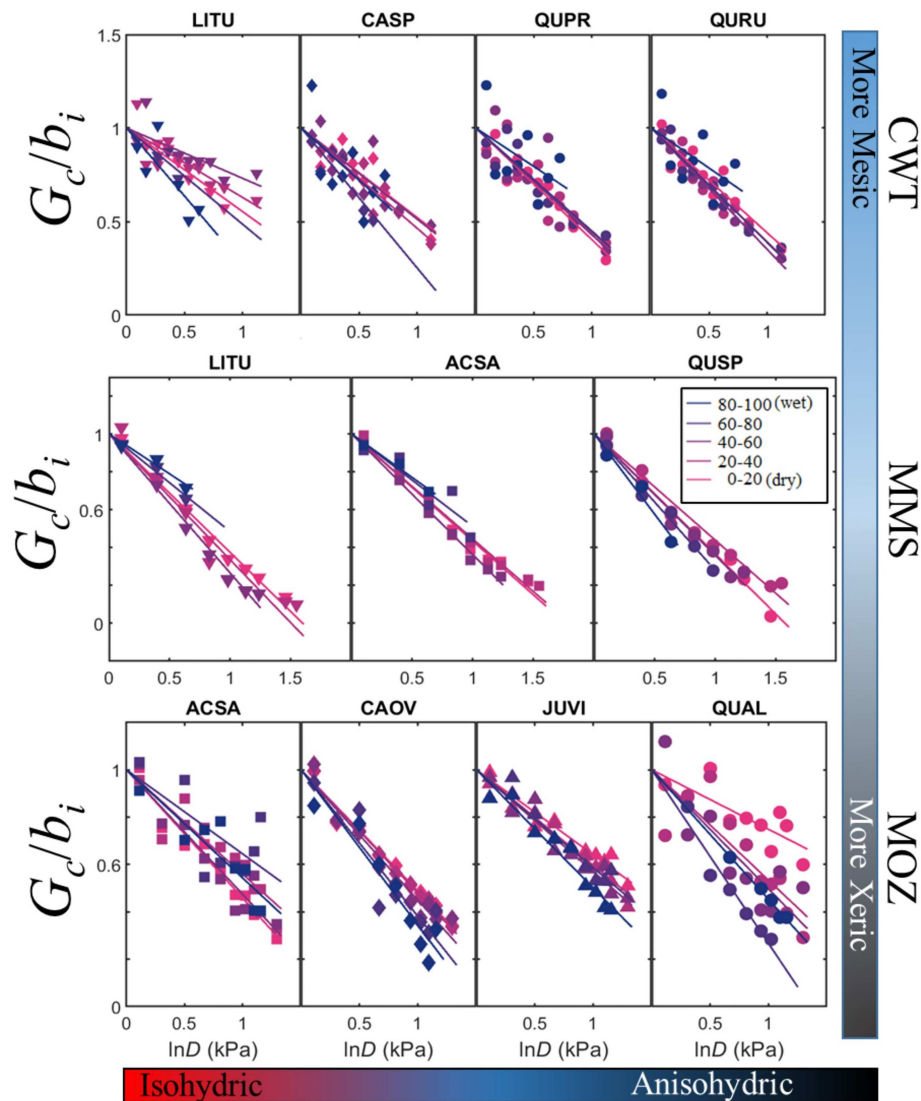


Figure 3. The normalized G_c , normalized by the intercept parameter within each soil moisture (%) bin, as a function of the natural logarithm of D . Data for each site CWT (top), MMS (middle) and MOZ (bottom) are listed for each tree species (see text for species codes).

The parameters of the G_c model (Eq. (7)) explained the shape of the observed relationships between Ψ_L and D at MMS. Initially, Ψ_L decreased linearly as D increased, but eventually a minimum Ψ_L was reached, around $D \sim 2.5$ kPa for isohydric LITU (Figure 8b) and ~ 3 kPa for anisohydric QUSP (Figure 8a). Beyond this point, Ψ_L tended to increase with increasing D . This pattern was clearly predicted by Eq. (7) when driven by the empirical stomatal sensitivities (m) and degree of isohydricity (c_{gk}) determined from the data. While Ψ_L decreased linearly with increasing D to a point, at high values of D , the relationship changed. In MOZ, the observed relationship between Ψ_L and D was, overall, more linear for all species (Figure 8c–f); likewise, the model predicted a more linear relationship between Ψ_L and D (Figure 8i–l).

Discussion

Our main goal was to determine if the sensitivity of G_c to D varied in a predictable way across species and sites, focusing especially on how variable θ affected this sensitivity. Overall, we found that the sensitivity of G_c to D was predictable from the sensitivity of G_c to θ . Specifically, the ratio of the slope and intercept parameters of Eq. (1) (m/b) was generally well conserved across sites and species, regardless of θ condition or the species-specific hydraulic trait (i.e., isohydricity, Figures 4 and 5). The G_c sensitivity to θ , interpreted as within-site variation in G_c , varied considerably across sites. However, we observed a high degree of convergence in the stomatal sensitivity to D once soil moisture effects were accounted for, at least within a site (Figure 3). In other words, the D sensitivity tracked the

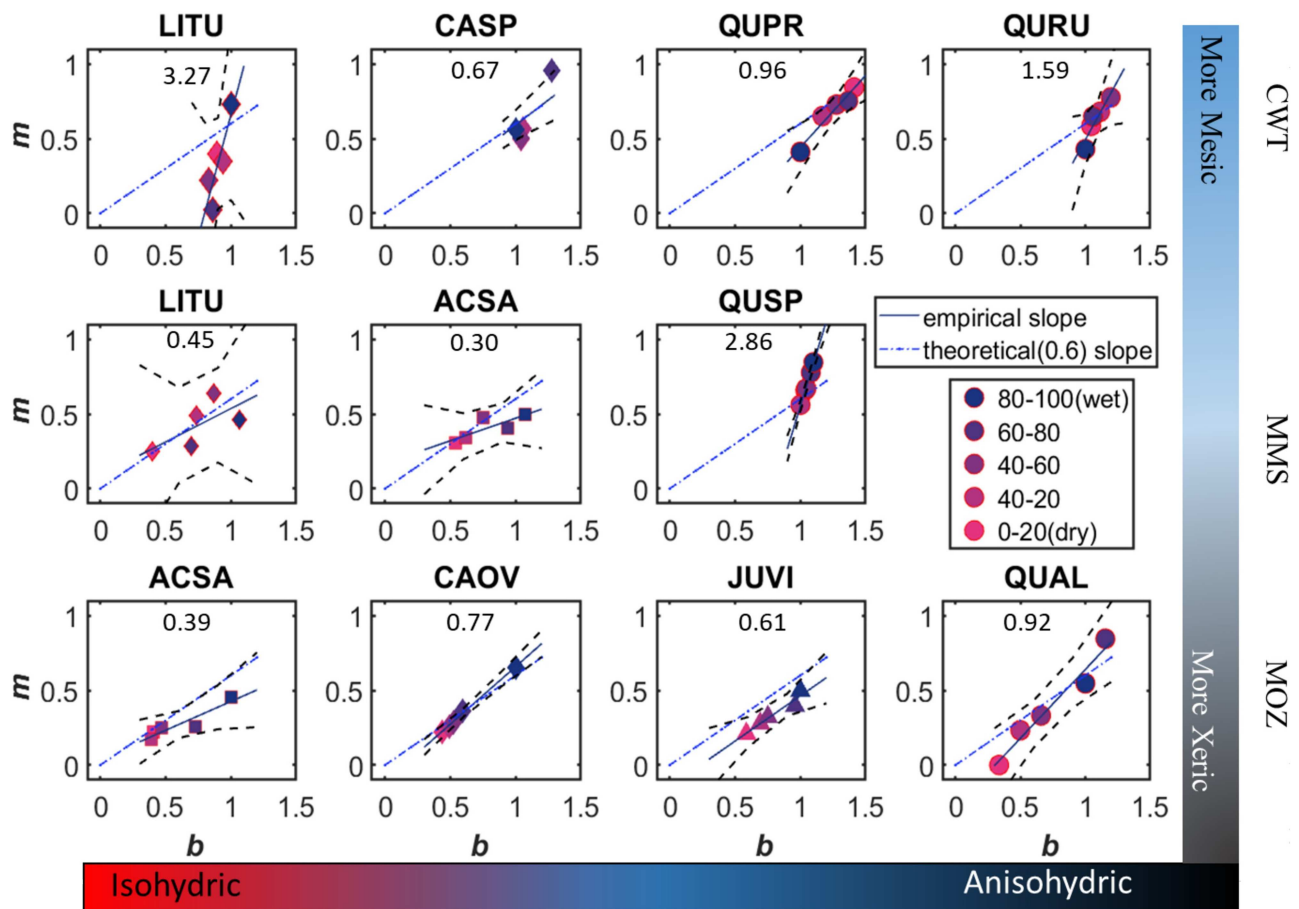


Figure 4. Relationship model parameters derived from Oren et al. (1999) (solid line) with 95% confidence bounds (dashed black lines) compared with the theoretical slope of 0.6 (dashed blue line). Although, in most circumstances, species tend to follow the theoretical slope, LITU in CWT demonstrates variable sensitivity to D even when maintaining high G_c . Empirical slopes indicated within each panel.

θ sensitivity, which was captured as variation in the intercept parameter of Eq. (1). This result extends the findings of Oren et al. (1999) to a broader range of θ conditions. Just as the relative sensitivity of G_c to D was fairly generalizable across species during well-watered conditions, we found that it was relatively applicable across all θ conditions. It is important to note, however, that the oaks of MOZ appeared to behave differently than the oaks of CWT and MMS, where we observed a sharper decrease in G_c sensitivity to D with declining θ .

We also sought to understand overall how much of the limitation to G_c during the growing season was driven by D and θ , both of which varied in importance in limiting G_c across sites. All species were clearly affected by D , in all study sites. Not surprisingly, the G_c of the more isohydric species—LITU, ACSA and even CAO V—were substantially limited by θ . Specifically, in MMS, LITU and ACSA experienced considerable θ limitation (>50%) during drought, reflected as variable intercepts in Figure 3; however, oak G_c was virtually unaffected by θ , even during the drought of 2012. On the contrary, in MOZ, G_c of each species, including the more anisohydric QUAL and JUVI, was limited by θ (Figure 6c), possibly due to thin soils that

characterized this oak–hickory forest, which could exacerbate plant water stress (Gu et al. 2015).

Our results revealed that stomatal sensitivity to D was not clearly related to hydraulic strategy (i.e., degree of isohydricity; Figure 7b and c). In other words, species whose G_c was sensitive to changes in θ (e.g., isohydric) did not also exhibit an increased G_c sensitivity to D after controlling for θ -driven changes in the intercept. This result is interesting in the context of the broader isohydricity framework, as some studies on the topic have suggested that species that tightly control stomatal conductance as soil water declines also more tightly regulate stomata as D rises (Hochberg et al. 2018, Novick et al. 2019). However, our results could not find any compelling evidence to support this conclusion.

In what may initially appear to be a paradox, despite the fact that there was no clear relationship between m and σ_S or σ_D (Figure 7a and b), we observed a linear relationship between σ_S and σ_D (Figure 7c). In fact, the model of Eq. (7) predicts this. For two species that experience the same D and Ψ_S , and that have the same m/b , the theory predicts a greater sensitivity of Ψ_L to D for a more anisohydric species (i.e., one with low c_{gk}).

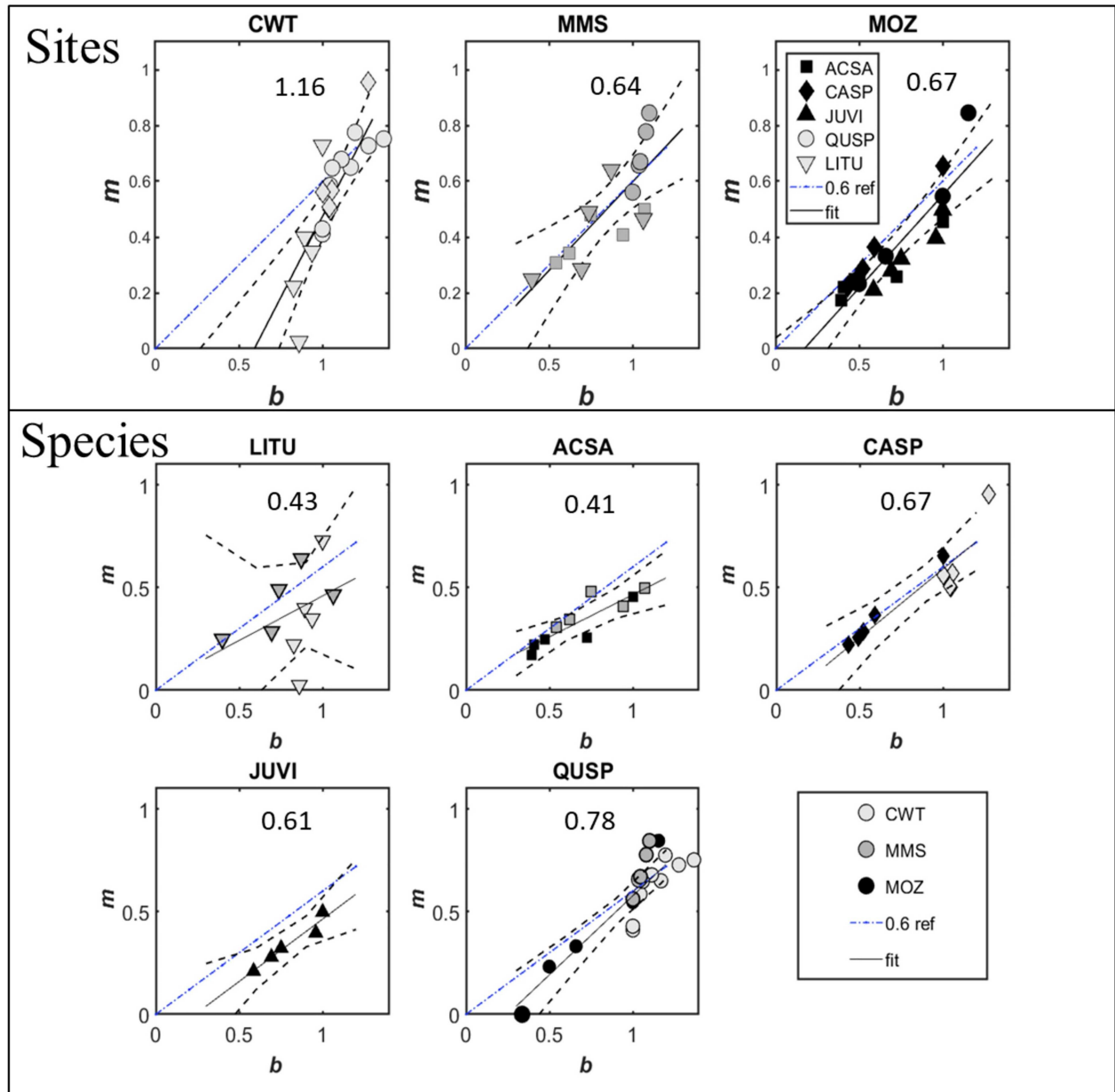


Figure 5. Similar to Figure 4, but pooling data across sites and species. Relationship model parameters derived from Oren et al. (1999) (solid line) with 95% confidence bounds (dashed black lines) compared with the theoretical slope of 0.6 (dashed blue line). Empirical slopes indicated within each panel. Species follow species symbols: ACSA (squares), *Carya* spp. (diamonds), LITU (downward triangles), JUVI (upward triangles) and *Quercus* spp. (circles); sites follow color: CWT (open), MMS (gray) and MOZ (black).

This reflects the fact that stomata are simply more open when D is high for anisohydric species, exposing these species to greater tensions in the leaf and stem as water is lost more rapidly to dry air. This further supports the notion that true isohydricity maintains Ψ_L within as narrow a range as possible as a variety of environmental conditions change, as is also described in Hochberg et al. (2018) and Tardieu and Simonneau (1998).

Stomatal sensitivity to D (i.e., m) explained the non-linear relationship between Ψ_L and D , especially during dry θ conditions (Figure 8). This was demonstrated by using Eq. (7),

driven by the empirically derived model parameters (m/b and c_{gk}). Specifically, at least in MMS, while Ψ_L initially decreased as D increased, eventually a minimum Ψ_L was reached, and then began to increase with increasing D as stomata closed. This result was mostly driven by the stomatal sensitivity to D , which has been often neglected in traditional applications of the isohydric framework. It can also at least partially explain the paradoxical result of 'shifting' degrees of isohydricity as drought evolves (Hochberg et al. 2018), given that D and θ are correlated over days and weeks (Novick et al. 2016).

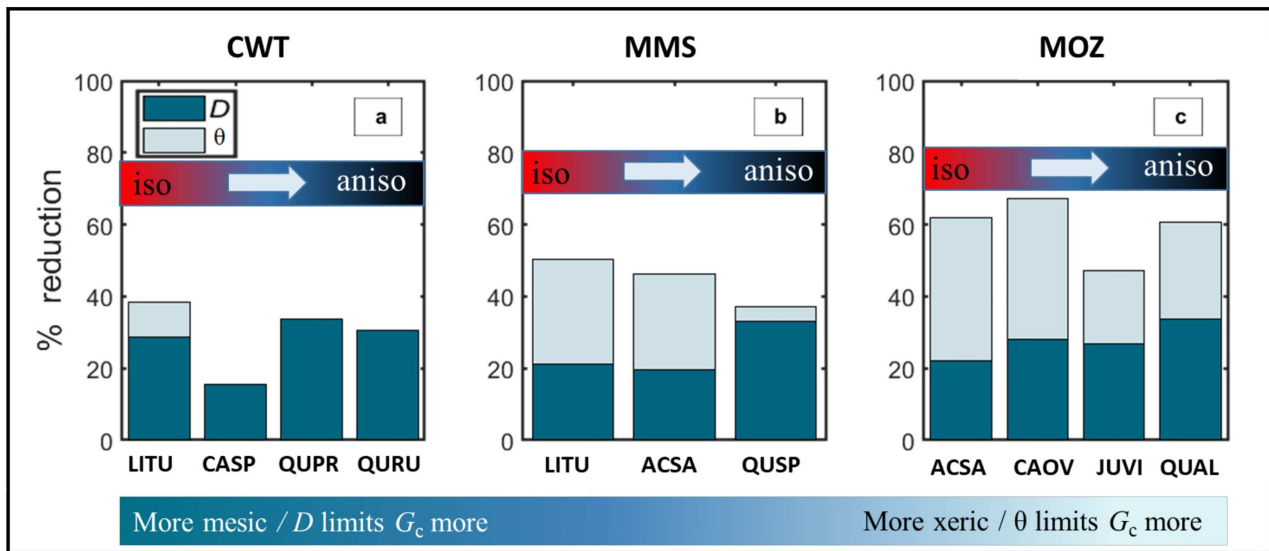


Figure 6. Limitations in normalized G_c attributed to D (dark bars) or to θ (light bars) for each tree species (see text for species abbreviations) at (a) Coweeta (CWT), (b) Morgan–Monroe State Forest (MMS) and (c) Missouri Ozark flux tower site (MOZ). Normalized G_c limitations are represented as a percent reduction from maximum G_c under well-watered conditions. Gradient color bar represents moving from more isohydric ('iso') to more aniso-hydric ('aniso') species.

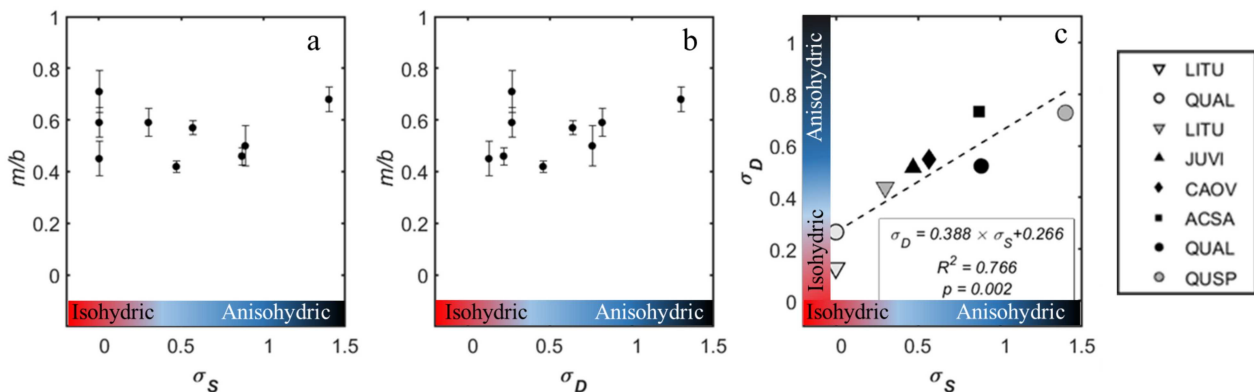


Figure 7. The relationship of the ratio m/b and σ_S (a) and σ_D (b), and the relationship between σ_S and σ_D (c). Error bars in (a) and (b) represent standard error of the mean. Panel (c) symbols: CWT (open), MMS (gray) and MOZ (black). Species symbols: LITU (downward triangle), all *Quercus* (circles), JUVI (upward triangle), ACSA (square) and CAO, V (diamond).

θ limitations within and across sites

The fraction of total G_c limitation attributable to θ varied across species and sites. In the driest site (MOZ), θ exhibited the greatest role in reducing G_c and progressively became less important, moving towards more mesic conditions (Figure 6). When comparing across species, within a site, θ was a more important regulator of G_c reductions in isohydric species than in aniso-hydric species within a site (as expected), but not necessarily when comparing an isohydric species of one site with an aniso-hydric species of another site. A fully coupled soil–plant–atmosphere continuum model presented by Tuzet et al. (2003) indicates that modeled stomatal conductance depends both on soil and plant hydraulic properties, which is further

illustrated by our results, highlighting the potential for model improvement when allowing parameterization of plants with differing stomatal control over Ψ_L . Though isohydric species in all sites experienced substantial reductions in G_c attributed to θ limitations, G_c of oaks in CWT and MMS were nearly unaffected by θ ; however, in MOZ (which also experienced a substantial dry period) G_c of both QUAL and JUVI was reduced by >50%. In other words, despite the fact that oaks are well known to be aniso-hydric, they experienced substantial limitation to G_c from θ in MOZ, as did eastern redcedar, also known to be a more drought tolerant species (Lowenstein and Pallardy 1998, Gu et al. 2015). Schäfer (2011) reports that drought conditions in 2006 caused reductions in G_c of three species

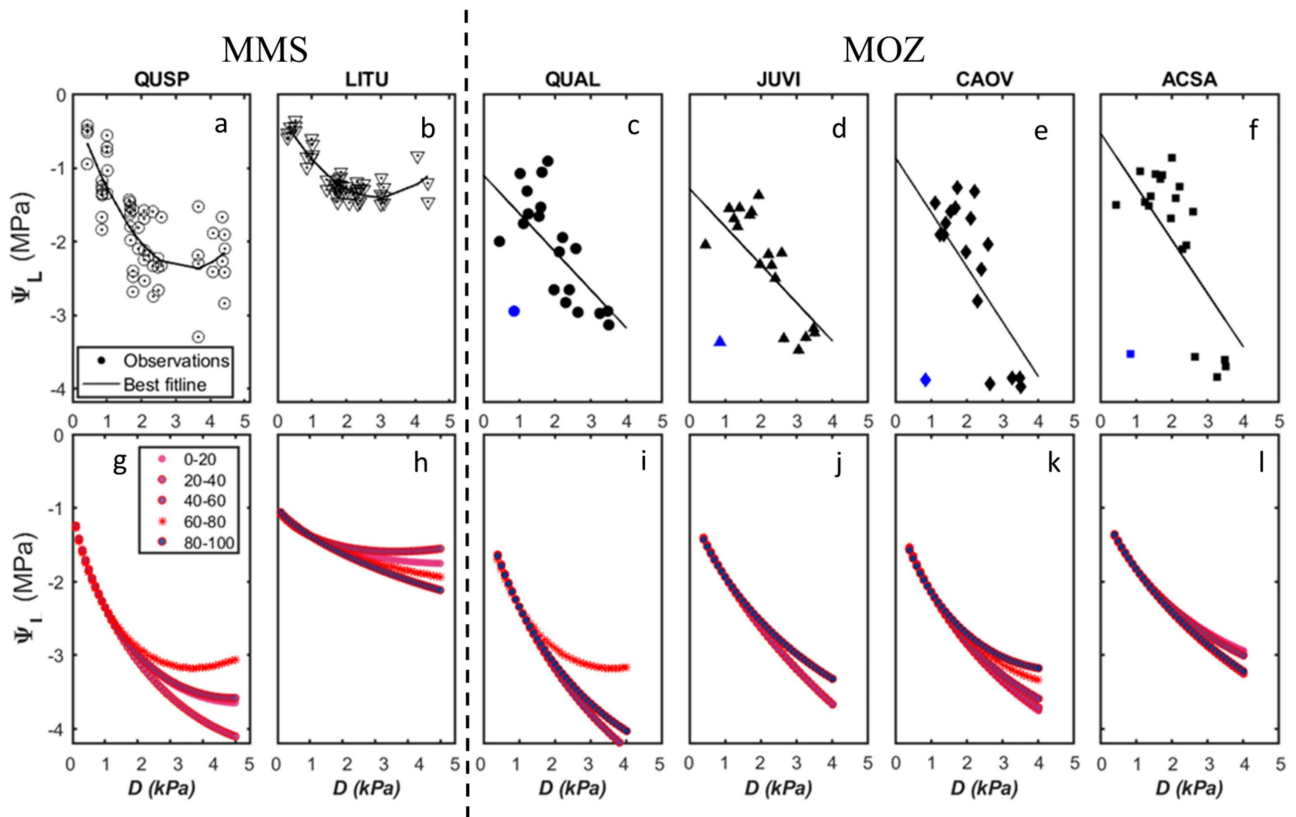


Figure 8. Ψ_L as a function of D to establish σ_D with regression (top, a–f) and theoretically modeled change in Ψ_L with increasing D using empirically derived c_{gk} and m parameters for each θ bin (bottom, g–l). Blue points in (c–f) represent abnormal observations that occurred in all MOZ species on the same day; however, these points were not excluded from the regression. Symbols in (a–f) correspond with the symbol convention of previous figures.

of oak (*Q. prinus*, *Q. coccinea* and *Q. velutina*) in the Pine Barrens of New Jersey, USA, which is an extremely water-limited environment (Schäfer 2011). This suggests that the species living in environments that are more frequently exposed to dry conditions, including those that typically have more risky water-use strategies, will respond to declining soil water availability by closing their stomata, which explains why even drought tolerant oaks in MOZ would demonstrate substantial reductions in G_c attributed to declining soil moisture. There is evidence suggesting that stomatal responses to D and θ involve a hydroactive component such as de novo biosynthesis of abscisic acid (ABA) in roots and leaves, which may help explain the differing results between MMS and MOZ (Khalil and Grace 1993). Thin soils characterizing the oak–hickory forest of MOZ would likely inhibit the depth to which roots could grow; thus oaks, thought to have access to deeper held soil water via deeper roots, may not have had access to deeper water in this site, resulting in roots being droughted, similar to other cohabiting species. This would initiate the ABA response signaling stomatal closure (Khalil and Grace 1993). On the contrary, in environments that rarely experience water-limitations, tree species that utilize a more risky water-use strategy (i.e., anisohydric species)

maintain relatively high stomatal conductance under these same conditions.

Stomatal sensitivity in response-changing θ environments

The conservation of the ratio m/b across θ conditions further reinforces the notion of functional convergence of responses to the environment (Meinzer 2003) and broadens the work of Oren et al. (1999) beyond well-watered conditions. High atmospheric demand reduces G_c more when θ is high; however, when θ limits G_c curves converge, consistent with Tuzet et al. (2003). We demonstrated that, generally speaking, stomatal sensitivity to D was proportional to the magnitude of G_c at low D for a range of species and sites (Figure 4), confirming other recent work on the topic (Drake et al. 2017). Specifically, after accounting for the reduction in G_c attributed to θ , we found that the G_c sensitivity to D remained relatively constant within and across species and sites (Figure 7). However, these results offer little insight into the responses of mechanisms such as stomatal density or intrinsic differences in guard cell behavior, which would allow a greater understanding of the convergence of physiological functioning within these comparable conditions (Meinzer 2003). The steepest slope in the relationship between

b and m was observed in CWT, which experienced very little θ limitation to G_c (e.g., b never falls below 0.88, Figure 5), and no difference in this relationship between MMS and MOZ. We observe no change in relative stomatal sensitivity to D with any changing θ and no inter-specific difference across species along the iso/anisohydric spectrum (featured in the slope between b and m). This is contrary to reports stating that the stomata of ring-porous species (e.g., oaks) were less responsive to D (Oren and Pataki 2001, Meinzer et al. 2013) but support the Oren et al. (1999) finding that stomatal sensitivity to D tracks proportionally with reference G_c .

Coordination between stomatal dynamics and Ψ_L

The traditional view of isohydricity predicts that Ψ_L declines linearly for anisohydric species, often to extremely negative values, while isohydric species maintain relatively constant Ψ_L for those same changes in Ψ_s (see Figure 2a). By using the expanded view, we are able to demonstrate that stomatal sensitivity to D promotes non-linear in the relationship between Ψ_L and Ψ_s for at least one isohydric (LITU, MMS) and one anisohydric (QUSP, MMS). However, the same result was not observed in MOZ, and more work is clearly needed to better understand how stomatal response to soil and atmospheric drought ultimately affect leaf water potential dynamics. Historically, questions like these have been challenging to address, given a relative paucity of Ψ_L observations, typically made on a small number of leaves on a weekly bases, especially when compared with the continuous, half-hourly resolution of sap flux data. Looking forward, one promising approach to overcome the Ψ_L data scarcity is the use of in-situ stem and leaf psychrometers (see Guo et al. 2019, for example), which provide an automated measurement of plant water potential at sub-hourly time scales.

The strong correlation observed between σ_S and σ_D (Figure 7) indicates that species which regulate their stomata in order to maintain Ψ_L within a narrow range as the soil dries (e.g., 'isohydric species' using the traditional definition) also sustain more constant Ψ_L in response to rising evaporative demand. Similarly, species that allow their Ψ_L to become increasingly negative with declining θ (i.e., 'anisohydric species') exhibit similar behavior in response to increasingly dry air. The coordination between σ_S and σ_D may be useful for characterizing degree of isohydricity in environments that do not experience a large range of Ψ_s during the growing season (Hochberg et al. 2018). In other words, the coordination implies that changes in Ψ_L with increasing D are predictive of expected changes in Ψ_L with decreasing soil water. As a result, opportunistic heat waves (accompanied by large ranges in D) may be used to characterize a species-specific water-use strategy, avoiding the need to wait for a well-established soil drought to accomplish the same goal.

Conclusions

With this work, we demonstrate that the stomatal sensitivity to D (i.e., m) tracks, and is predictable from, θ -driven reductions to b ; specifically, the ratio m/b is well conserved across sites, species and soil moisture conditions. Our study extends the primary conclusion of Oren et al. (1999) to variable θ conditions and includes species that have different water-use strategies. While G_c responses to θ condition vary, D emerges as a major driver of G_c reductions in all sites and species. However, functional convergence of G_c sensitivity to D occurs once θ limitations are accounted for across sites and species. These results suggest that under a future climate characterized by increasing D , we may see large reductions in G_c across many species, regardless of where they fall along the continuum of water-use strategy and independent of local edaphic conditions.

Funding

We acknowledge support from the US Department of Energy, through the Terrestrial Ecosystem Science Program and the AmeriFlux Management Project, the National Science Foundation, Division of Environmental Biology (grant DEB 1552747 and DEB 1637522), the USDA Agriculture and Food Research Initiative (grants 2012-67019-19484 and 2017-67013-26191) and NASA-ROSES Carboy Cycle Science (grant NNX17AE69G).

Conflict of interest

The authors declare that there is no conflict of interest.

References

- Améglio T, Archer P, Cohen M, Valancogne C, Daudet FA, Dayau S, Cruziat P (1999) Significance and limits in the use of predawn leaf water potential for tree irrigation. *Plant Soil* 207:155–167.
- Berg A, Sheffield J, Milly PC (2017) Divergent surface and total soil moisture projections under global warming. *Geophys Res Lett* 44:236–244.
- Choat B, Jansen S, Brodribb TJ et al. (2012) Global convergence in the vulnerability of forests to drought. *Nature* 491:752.
- Comstock J, Mencuccini M (1998) Control of stomatal conductance by leaf water potential in *Hymenoclea salsola* (T. & G.), a desert shrub. *Plant Cell Environ* 21:1029–1038.
- Domec JC, Noormets A, King JS, Sun G, McNulty SG, Gavazzi MJ, Boggs JL, Treasure EA (2009) Decoupling the influence of leaf and root hydraulic conductances on stomatal conductance and its sensitivity to vapor pressure deficit as soil dries in a drained loblolly pine plantation. *Plant Cell Environ* 32:980–991.
- Dragoni D, Caylor KK, Schmid HP (2009) Decoupling structural and environmental determinants of sap velocity: part II. Observational application. *Agric For Meteorol* 149:570–581.
- Drake JE, Power SA, Duursma RA et al. (2017) Stomatal and non-stomatal limitations of photosynthesis for four tree species under drought: a comparison of model formulations. *Agric For Meteorol* 247:454–466.

- Ficklin DL, Novick KA (2017) Historic and projected changes in vapor pressure deficit suggest a continental scale drying of the United States atmosphere. *J Geophys Res Atmos* 122:2061–2079.
- Ford CR, Hubbard RM, Vose JM (2011) Quantifying structural and physiological controls on variation in canopy transpiration among planted pine and hardwood species in the southern Appalachians. *Ecohydrol* 4:183–195.
- Franks PJ, Buckley TN, Shope JC, Mott KA (2001) Guard cell volume and pressure measured concurrently by confocal microscopy and the cell pressure probe. *Plant Physiol* 125:1577–1584.
- Gao J, Zhao P, Shen W, Niu J, Zhu L, Ni G (2015) Biophysical limits to responses of water flux to vapor pressure deficit in seven tree species with contrasting land use regimes. *Agric For Meteorol* 200:258–269.
- Granier A (1987) Evaluation of transpiration in a Douglas-fir stand by means of sap flow measurements. *Tree Phys* 3:309–320.
- Green S, Clothier B, Jardine B (2003) Theory and practical application of heat pulse to measure sap flow. *Agron J* 95:1371–1379.
- Grossiord C, Buckley TN, Cernusak LA, Novick KA, Poulter B, Siegwolf RT, Sperry JS, McDowell NG (2020) Plant responses to rising vapor pressure deficit. *New Phytol* 226:1550–1566.
- Gu L, Pallardy SG, Hosman KP, Sun Y (2015) Drought-influenced mortality of tree species with different predawn leaf water dynamics in a decade-long study of a central US forest. *Biogeosciences* 12:2831–2845.
- Guo JS, Hultine KR, Koch GW, Kropp H, Ogle K (2019) Temporal shifts in iso/anisohydry revealed from daily observations of plant water potential in a dominant desert shrub. *New Phytol*. 225(2). doi: [10.1111/nph.16196](https://doi.org/10.1111/nph.16196).
- Hochberg U, Rockwell FE, Holbrook M, Cochard H (2018) Iso/anisohydry: a plant-environment interaction rather than a simple hydraulic trait. *Trends Plant Sci* 23:112–120.
- Kennedy D, Swenson S, Oleson KW, Lawrence DM, Fisher R, Loda da Costa AC, Gentine P (2019) Implementing plant hydraulics in the community land model, version 5. *J Adv Model Earth Syst* 11:485–513.
- Khalil AAM, Grace J (1993) Does xylem sap ABA control the stomatal behavior of water-stressed sycamore (*Acer pseudoplatanus* L.) seedlings? *J Exp Bot* 44:1127–1134.
- Klein T (2014) The variability of stomatal sensitivity to leaf water potential across tree species indicates a continuum between isohydric and anisohydric behaviors. *Funct Ecol* 28:1313–1320.
- Konings AG, Gentine P (2017) Global variations in ecosystem-scale isohydricity. *Glob Chang Biol* 23:891–905.
- Lowenstein NJ, Pallardy SG (1998) Drought tolerance, xylem sap abscisic acid and stomatal conductance during soil drying: a comparison of canopy trees of three temperate deciduous angiosperms. *Tree Physiol* 18:431–439.
- Maier-Maercker U (1999) New light on the importance of peristomatal transpiration. *Funct Plant Biol* 26:9–16.
- Martinez-Vilalta J, Poyatos R, Aguade D, Retena J, Mencuccini M (2014) A new look at water transport regulation in plants. *New Phytol* 204:105–115.
- Massman WJ, Kaufmann MR (1991) Stomatal response to certain environmental factors: a comparison of models for subalpine trees in the Rocky Mountains. *Agric For Meteorol* 54:155–167.
- McDowell N, Pockman WT, Allen CD et al. (2008) Mechanisms of plant survival and mortality during drought: why do some plants survive while others succumb to drought? *New Phytol* 178:719–739.
- Meinzer FC (2003) Functional convergence in plant responses to the environment. *Oecologia* 134:1–11.
- Meinzer FC, Woodruff DR, Eissenstat DM, Lin HS, Adams TS, McCulloh KA (2013) Above- and belowground controls on water-use by trees of different wood types in an eastern US deciduous forest. *Tree Phys* 33:345–356.
- Mirfenderesgi G, Matheny AM, Bohrer G (2019) Hydrodynamic trait coordination and cost-benefit trade-offs throughout the isohydric – anisohydric continuum in trees. *Ecohydrology* 12:1–16.
- Monteith JL (1995) A reinterpretation of stomatal response to humidity. *Plant Cell Environ* 18:357–364.
- Mott KA, Franks PJ (2001) The role of epidermal turgor in stomatal interactions following a local perturbation in humidity. *Plant Cell Environ* 24:657–662.
- Mott KA, Parkhurst DF (1991) Stomatal responses to humidity in air and helox. *Plant Cell Environ* 14:509–515.
- Novick KA, Ficklin DL, Stoy PC et al. (2016) The increasing importance of atmospheric demand for ecosystem water and carbon fluxes. *Nat Clim Change* 6:1023–1027.
- Novick KA, Konings AG, Gentine P (2019) Beyond soil water potential: an expanded view on isohydricity including land-atmosphere interactions and phenology. *Plant Cell Environ* 42.
- Oren R, Pataki DE (2001) Transpiration in response to variation in microclimate and soil moisture in southeastern deciduous forests. *Oecologia* 127:549–559.
- Oren R, Sperry JS, Katul GG, Pataki DE, Ewers BE, Phillips N, Schäfer KVR (1999) Survey and synthesis of intra- and interspecific variation in stomatal sensitivity to vapour pressure deficit. *Plant Cell Environ* 22:1515–1526.
- Osonubi O, Davies WJ (1980) The influence of plant water stress on stomatal control of gas exchange at different levels of atmospheric humidity. *Oecologia* 46:1–6.
- Renninger HJ, Carlo NJ, Clark KL, Scafer KVR (2015) Resource use and efficiency, and stomatal responses to environmental drivers of oak and pine species in an Atlantic coastal plain forest. *Front Plant Sci* 6:1–16.
- Roman DT, Novick KA, Brzostek ER, Dragoni D, Rahman F, Phillips RP (2015) The role of isohydric and anisohydric species in determining ecosystem-scale response to severe drought. *Oecologia* 179:641–654.
- Schäfer KVR (2011) Canopy stomatal conductance following drought, disturbance, and death in an upland oak/pine forest of the New Jersey pine barrens, USA. *Front Plant Sci* 2:1–7.
- Swank WT, Swift LW Jr, Douglass JE (1988) Introduction and site description. In: Swank WT, Crossley DA Jr (eds) *Forest hydrology and ecology at Coweeta*. Ecological studies, Vol. 66. Springer, New York, NY, pp 3–17.
- Tardieu F, Simonneau T (1998) Variability among species of stomatal control under fluctuating soil water status and evaporative demand: modelling isohydric and anisohydric behaviours. *J Exp Bot* 49:419–432.
- Tuzet A, Perrier A, Leuning R (2003) A coupled model of stomatal conductance, photosynthesis and transpiration. *Plant Cell Environ* 26:1097–1116.
- Tyree MT, Sperry JS (1989) Vulnerability of xylem to cavitation and embolism. *Annu Rev Plant Phys Mol Bio* 40:19–38.
- Whitehead D, Edwards WRN, Jarvis PG (1984) Conducting sapwood area, foliage area, and permeability in mature trees of *Picea sitchensis* and *Pinus contorta*. *Can J For Res* 14:940–947.
- Wood JD, Knapp BO, Muzika R, Stambaugh MC, Gu L (2018) The importance of drought-pathogen interactions in driving oak mortality events in the Ozark border region. *Env Res Lett* 13:1–11.
- Wullschlegel SD, Hanson PJ, Todd DE (2001) Transpiration from a multispecies deciduous forest as estimated by xylem sap flow techniques. *For Ecol Manage* 143:205–213.
- Yi K, Dragoni D, Phillips RP, Roman DT, Novick KA (2017) Dynamics of stem water uptake among isohydric and anisohydric species experiencing a severe drought. *Tree Phys* 37:1–14.